JPPIPA 12(1) (2026)

Jurnal Penelitian Pendidikan IPA

http://jppipa.unram.ac.id/index.php/jppipa/index

Remote Sensing for Sustainable Development: Multi-Temporal Landsat Analysis of Land-Use Change and Urbanization in the Rejoso Watershed (2005–2024)

Alyavara Mayang Ferynandari[1*], Ery Suhartanto[2], Linda Prasetyorini[2]

[1] Master Program of Water Resources Engineering, Universitas Brawijaya, Malang, Indonesia.
[2] Department of Water Resources Engineering, Universitas Brawijaya, Malang, Indonesia.

Received: November 28, 2025
Revised: December 23, 2025
Accepted: January 25, 2026
Published: January 31, 2026

Corresponding Author:
Alyavara Mayang Ferynandari
alyavaraferynandari@gmail.com

DOI: 10.29303/jppipa.v12i1.13639

Abstract: Rapid urbanization and shifting agricultural practices are reshaping watershed sustainability in Indonesia, yet their spatial and hydrological implications in the Rejoso Watershed (East Java) remain insufficiently quantified. This study evaluates land-use/land-cover (LULC) dynamics over 2005–2024 using multi-temporal Landsat imagery from five observation years (2005, 2011, 2015, 2020, and 2024). A hybrid classification (ISODATA clustering combined with visual interpretation) was validated using 250 ground points and confusion matrix metrics (overall accuracy and Kappa). Vegetation declined from 54.72% (197.11 km²) in 2005 to its minimum in 2020 at 38.06% (137.09 km²), then recovered to 41.28% (148.70 km²) in 2024. Agricultural land expanded from 32.14% (115.77 km²) to 52.28% (188.32 km²) in 2020 before contracting to 46.96% (169.14 km²) in 2024, indicating a notable post-2020 trend reversal with vegetation regrowth and reduced cropland extent. Built-up areas increased steadily (4.14% to 7.54%), while open land fluctuated and water bodies remained <1% with a slight decline. The 2020 map achieved the highest accuracy (95.83%; κ=0.96). These findings highlight upstream LULC reconfiguration and continued downstream urbanization, supporting integrated watershed management, upland rehabilitation, and stricter spatial planning.

Keywords: Land-use change; Multi-temporal landsat; Rejoso watershed; Remote sensing; Spatial dynamics

Introduction

The pattern of land use and land cover (LULC) change has become a defining feature of watershed transformation across Indonesia and Southeast Asia, driven by rapid urbanization, agricultural intensification, and infrastructure expansion. Numerous studies in comparable tropical watersheds report recurring patterns in which vegetated areas are converted into cropland or settlements, often producing fragmented landscapes and increasing pressure on ecosystem services. In Indonesian settings such as the Plumbon and Biyonga Watersheds, demographic growth and peri-urban development have been associated with vegetation degradation and shifts toward more intensive land uses, while similar dynamics across Southeast Asia indicate that expanding human land demands can weaken landscape capacity for water retention and soil stabilization (Budiman et al., 2022; Ogato et al., 2021). Recent studies in Southeast Asia also emphasize that rapid peri-urban expansion has accelerated the conversion of agricultural and vegetated land, causing regional-scale declines in water retention and soil stability (Aboelnour et al., 2024).

However, despite these evident transformations, the magnitude and spatial pattern of land-use change in the Rejoso Watershed have not been systematically quantified. Previous research has primarily examined similar phenomena in other Indonesian watersheds but has lacked a detailed multi-temporal assessment

How to Cite:
Ferynandari, A. M., Suhartanto, E., & Prasetyorini, L. Remote Sensing for Sustainable Development: Multi-Temporal Landsat Analysis of Land-Use Change and Urbanization in the Rejoso Watershed (2005–2024). *Jurnal Penelitian Pendidikan IPA*, *12*(1), 93-101. https://doi.org/10.29303/jppipa.v12i1.13639

specifically for Rejoso. Therefore, this study aims to analyze the spatiotemporal dynamics of land-use change from 2005 to 2024 and evaluate their environmental and hydrological impacts using multi-temporal Landsat imagery (Budiman et al., 2022; Yesuph & Dagnew, 2019).

The main drivers of LULC change in watersheds like Rejoso typically include population growth, rural-to-urban transition, and rising demand for housing, roads, and productive land. These drivers frequently create competition between agriculture and settlements, producing complex mosaics that are difficult to monitor without consistent satellite observation. Using multi-temporal Landsat imagery offers an effective way to trace these long-term dynamics because it provides continuous, standardized coverage suited for detecting gradual transitions and episodic disturbances (Fajri et al., 2025; Yusoff & Muharam, 2015). At a broader scale, land-use change has been recognized as a major contributor to hydrological alteration in tropical basins, emphasizing the need for watershed-specific monitoring that links spatial transitions to water-system sensitivity (Vigiak et al., 2015).

Urbanization- and agriculture-driven conversions can alter ecological and hydrological functioning by reducing infiltration zones, increasing impervious surfaces, and disturbing soil structure. Evidence from tropical watershed modeling indicates that such transitions may intensify runoff response, elevate peak discharge, and accelerate flow concentration, particularly where vegetation loss and settlement growth occur simultaneously (Aboelnour et al., 2024). These findings suggest that understanding LULC pathways is not only a land-management concern but also a hydrological risk issue, especially under monsoonal rainfall regimes (Octaviani et al., 2025).

The implications of LULC change in Rejoso are expected to extend from landscape degradation to shifts in watershed water balance, flood susceptibility, erosion potential, and the stability of agricultural productivity (Sadhwani et al., 2022). For rapidly developing Indonesian watersheds, sustainable management depends on recognizing where and how land transitions occur, then embedding that evidence into spatial planning and conservation priorities. Lessons from other watershed management experiences in Indonesia highlight that integrating ecological protection with land-use regulation is essential to maintain long-term watershed resilience (Budiman et al., 2022; Rachman et al., 2024).

This study contributes to LULC research in Indonesia in two key ways. First, it provides the first dedicated, multi-temporal, watershed-scale LULC assessment for Rejoso spanning nearly two decades, enabling identification of dominant transition pathways and their spatial hotspots. Second, it applies a hybrid classification framework with rigorous accuracy validation to improve class separability in a heterogeneous tropical landscape, offering a replicable approach for long-term monitoring. By linking multi-decadal remote-sensing evidence to watershed sustainability questions, the study delivers scientific insights to support adaptive land-use policy in rapidly urbanizing and agriculturally intensified regions.

Method

Study Area

The Rejoso Watershed (±360.21 km²) is located within the Welang–Rejoso Basin, Pasuruan Regency, East Java (112°33′55″–113°30′37″E; 7°32′34″–8°30′20″S). The watershed originates in the volcanic uplands near Mount Bromo and flows northward to the Java Sea (Figure 1). It comprises steep upland slopes in the south and lowland alluvial plains in the north, resulting in heterogeneous topography and diverse land-use patterns.

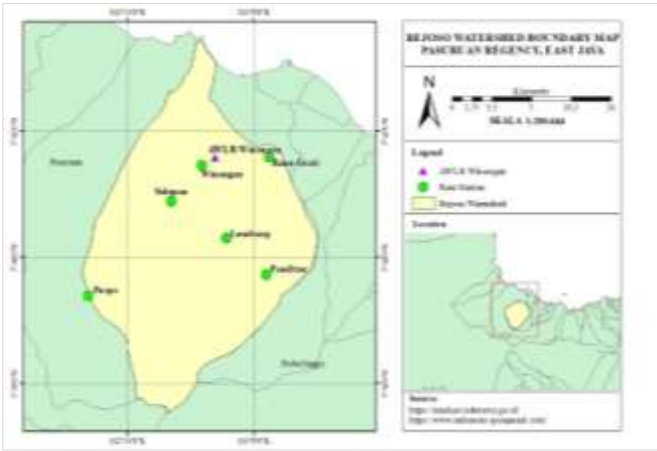

Figure 1. Rejoso Watershed

Data and Methodology

Five multi-temporal Landsat scenes were used, including Landsat 7 (ETM+) imagery for 2005, 2011, and 2015, and Landsat 8 (OLI/TIRS) imagery for 2020 and 2024, all with a spatial resolution of 30 m. All scenes (Path/Row 118/65) were acquired from USGS EarthExplorer and selected to ensure cloud cover below 5% (Adhikari et al., 2025; Groeneveld et al., 2024).

Image pre-processing included radiometric and atmospheric correction using the Dark Object Subtraction (DOS) method (Chavez & others, 1996), geometric correction and reprojection to UTM Zone 49S (WGS-84), and cloud masking to maintain temporal consistency. The corrected images were clipped to the watershed boundary and stacked into multi-band spectral composites. This approach enables

simultaneous processing of spectral information and reduces class confusion in heterogeneous landscapes (Yang et al., 2021).

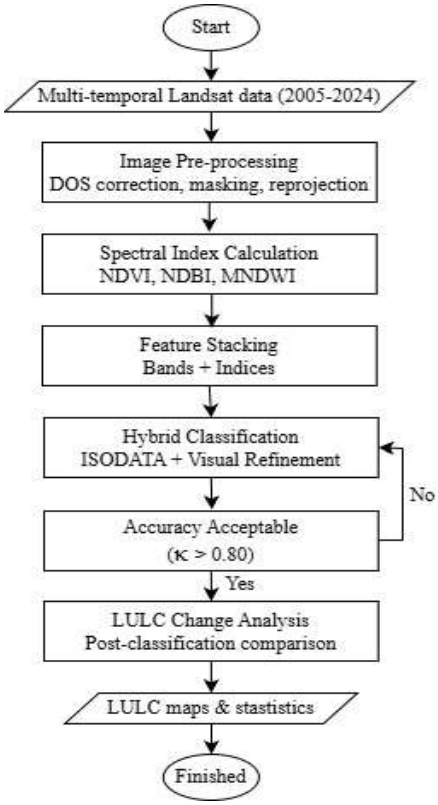

Figure 2. Research flow chart

Classification and Accuracy Validation

A hybrid classification approach combining unsupervised ISODATA clustering and visual interpretation was applied to optimize land-cover separability (Lu et al., 2004). ISODATA clustering was performed on stacked spectral bands augmented with spectral index layers (see Derived Indices section) to generate preliminary clusters. These clusters were subsequently interpreted and labeled into five land-use/land-cover (LULC) classes: Vegetation, Agricultural land, Built-up area, Open land, and Water bodies, based on their spectral behavior, index values, spatial patterns, and reference imagery (Khafaji & Al-Zubaidi, 2024).

Visual interpretation using false-color composites and spectral index layers was conducted to refine class boundaries and correct misclassified pixels, particularly in areas with high spectral similarity between agricultural land, open land, and sparsely vegetated surfaces. All classification procedures were implemented in ENVI 5.6 and ArcGIS 10.8 (Aravena et al., 2021).

A total of 250 ground-truth points were collected using GPS during field surveys and supplemented with visual interpretation of high-resolution Google Earth Pro imagery. The samples were proportionally stratified across LULC classes. Classification accuracy was evaluated using a confusion matrix to derive producer's accuracy, user's accuracy, overall accuracy, and the Kappa coefficient (Congalton, 1991). Kappa values greater than 0.80 were considered indicative of very high classification reliability. Previous studies have demonstrated that integrating spectral indices such as NDVI, NDBI, and MNDWI as classification inputs can improve accuracy in tropical environments (Xu et al., 2018).

Derived Indices

Three spectral indices—NDVI, NDBI, and MNDWI—were calculated for each Landsat scene to enhance class discrimination and support the hybrid classification process (McFeeters, 1996; Quilbé et al., 2008; Zha et al., 2003). The Normalized Difference Vegetation Index (NDVI) was used to quantify vegetation density and degradation.

$$NDVI = (NIR - Red)/(NIR + Red) \quad (1)$$

The Normalized Difference Built-up Index (NDBI) was used to detect impervious and urban surfaces.

$$NDBI = (SWIR - NIR)/(SWIR + NIR) \quad (2)$$

The Modified Normalized Difference Water Index (MNDWI) was applied to identify open-water bodies.

$$MNDWI = (Green - SWIR)/(Green + SWIR) \quad (3)$$

These indices provided auxiliary variables for verifying classification boundaries and interpreting land-use changes affecting hydrology.

Table 1. Data Used in the Study

Satellite Data	Path & Row	Spatial Resolution (m)	Data Acquired	Cloud Coverage	Source
Landsat 7 (ETM+)	118/65	30 m (Visible, NIR,	2/10/2005	<5%	https://earthexplorer.usgs.gov
Landsat 7 (ETM+)		SWIR), 15 m	1/9/2011		
Landsat 7 (ETM+)		(Panchromatic)	16/06/2015		
Landsat 8 (OLI TIRS)			3/10/2020		
Landsat 8 (OLI TIRS)			19/08/2024		

Land Transition and Spatial Analysis

Land-use change detection was conducted using post-classification comparison, which minimizes the influence of sensor-related spectral differences across multi-temporal Landsat datasets. Transition matrices were generated to quantify conversions among LULC classes, such as vegetation to agricultural land or agricultural land to built-up areas (Singh et al., 2018; Surbakti et al., 2025).

Spatial overlay analysis in ArcGIS was subsequently applied to calculate area and percentage changes for each LULC class and to identify hotspots of land-use transformation. Spectral indices, particularly NDVI and NDBI, were further used to support the interpretation of land-use transitions and associated hydrological implications, including changes in infiltration potential and surface sealing (Purwanto, 2023; Vahreza et al., 2024).

All procedures followed reproducible workflows based on open-access Landsat data and standard remote sensing algorithms, with data and processing details available upon request to ensure transparency and reproducibility (Ode et al., 2025; Singh, 1989).

Results and Discussion

Land Use and Land Cover Dynamics (2005–2024)

The Rejoso Watershed experienced pronounced multi-temporal land use and land cover (LULC) transitions between 2005 and 2024 (Figure 2; Table 2). Vegetation cover declined steadily from 54.72% (197.11 km²) in 2005 to 49.69% (178.99 km²) in 2011 and 44.08% (158.79 km²) in 2015, reaching its minimum extent in 2020 at 38.06% (137.09 km²). This sustained decline reflects progressive conversion of vegetated areas into other land uses, predominantly agriculture. In contrast, the 2024 classification shows an increase in vegetation to 41.28% (148.70 km²), representing a recovery of 3.22% (11.61 km²) relative to 2020. This rebound indicates partial re-vegetation, most likely associated with secondary vegetation regrowth on fallow agricultural land, marginal slopes, or previously degraded areas rather than full restoration of original forest cover. Agricultural land expanded markedly over most of the study period, increasing from 32.14% (115.77 km²) in 2005 to 36.99% (133.23 km²) in 2011 and 41.06% (147.90 km²) in 2015, before peaking in 2020 at 52.28% (188.32 km²). This expansion coincided with the sharpest decline in vegetation and open land, indicating that both classes served as the principal sources of agricultural growth. In 2024, agricultural land decreased to 46.96% (169.14 km²), a reduction of 5.32% (19.18 km²) compared with 2020. Given that built-up areas increased only marginally over the same period (from 7.46% to 7.54%), conversion to settlement cannot account for most of this decline. Instead, the reduction in agricultural land corresponds closely with the observed increase in vegetation (3.22%) and the renewed expansion of open land (from 1.70% to 3.77%), indicating a redistribution of agricultural areas into fallow land, temporarily abandoned fields, and zones undergoing natural regrowth. Built-up areas increased steadily and monotonically throughout the study period, from 4.14% (14.90 km²) in 2005 to 6.01% (21.64 km²) in 2011, 7.00% (25.22 km²) in 2015, 7.46% (26.86 km²) in 2020, and 7.54% (27.16 km²) in 2024, reflecting continuous settlement expansion and infrastructure development. Although persistent, the magnitude of built-up growth remains modest relative to agricultural expansion and thus represents a secondary driver of overall land-cover change. Open land exhibited a non-linear trajectory, declining from 8.02% (28.90 km²) in 2005 to 6.48% (23.36 km²) in 2011, increasing slightly in 2015 (7.24%; 26.08 km²), and then contracting sharply to 1.70% (6.13 km²) in 2020. This contraction indicates widespread conversion of bare or degraded surfaces into agricultural land during the peak expansion phase. The subsequent increase in open land to 3.77% (13.59 km²) in 2024 suggests renewed soil exposure, likely linked to short-term agricultural abandonment, land preparation cycles, or localized degradation. Water bodies remained the smallest LULC class and declined gradually from 0.98% (3.53 km²) in 2005 to 0.45% (1.63 km²) in 2024. Collectively, these trends demonstrate a long-term redistribution from vegetated landscapes toward agricultural dominance, followed by partial reorganization after 2020, consistent with land-use intensification dynamics reported in other monsoonal and tropical basins (Bal et al., 2023).

These quantitative changes indicate that watershed transformation in Rejoso is governed by two coupled processes: (i) sustained conversion of vegetation and open land into agriculture up to 2020, and (ii) post-2020 land-use reconfiguration characterized by partial agricultural contraction, vegetation regrowth, and renewed bare-land exposure. Post-classification comparison suggests that vegetation loss was the dominant source of agricultural expansion during earlier periods, while the decline in agricultural land after 2020 was primarily redistributed into vegetated and open-land classes rather than built-up areas. This pattern reflects cyclical land-use dynamics typical of intensively managed tropical watersheds, where phases of rapid agricultural expansion are followed by temporary abandonment and natural regrowth driven by land management adjustments and environmental constraints (Budiman et al., 2022; Yang et al., 2018).

Spatial Distribution and Hotspots of Change

The sharp contraction of open land in 2020 indicates that many previously bare or degraded areas were absorbed into agriculture during the peak expansion phase. Conversely, the re-emergence of open land in 2024 highlights renewed soil exposure, likely associated with rotational clearing, short-term abandonment, or localized degradation (Pandey et al., 2021). These spatially clustered transitions emphasize the heterogeneous and dynamic nature of land-use change within the Rejoso Watershed.

Consistent with findings from other watershed studies, widespread conversion of vegetated cover and episodic increases in bare land can reduce soil water retention and increase runoff sensitivity, particularly under intense rainfall conditions (Zhang et al., 2018). The spatial concentration of settlement growth in downstream areas combined with alternating bare-land hotspots upstream underscores the importance of prioritizing downstream zoning control and upstream slope protection to mitigate hydrological risk (Ogato et al., 2021).

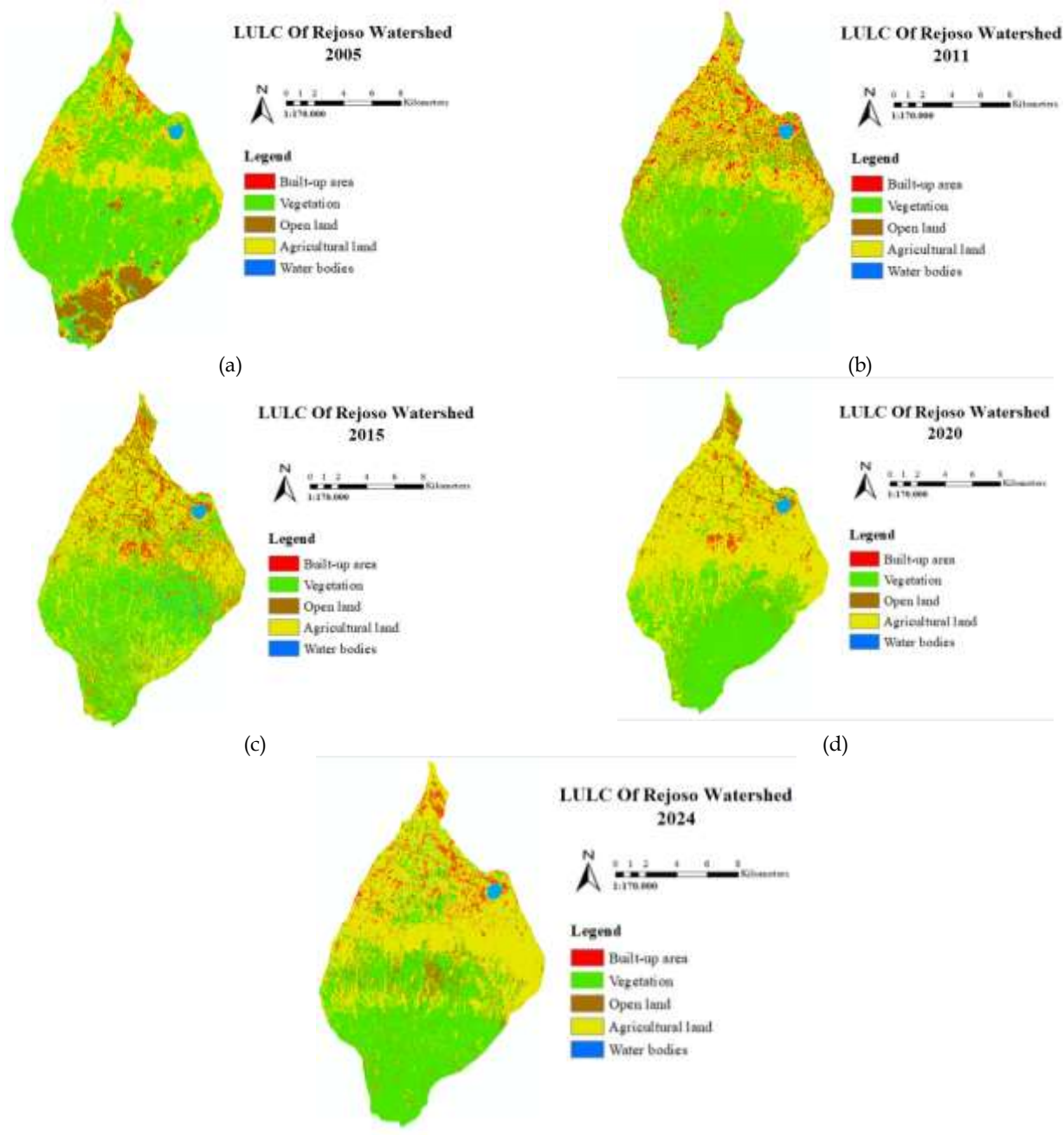

Figure 3. Land use/Land Cover Changes in: (a) 2005; (b) 2011; (c) 2015; (d) 2020; and (e) 2024

Table 2. Spatial Changes in Different Land Use/Land Cover Classes in The Study Area Between 2005 and 2024

LULC Classes	2005		2011		2015		2020		2024	
	km²	%	km²	%	km²	%	km²	%	km²	%
Water bodies	3.53	0.98	3.00	0.83	2.22	0.62	1.80	0.50	1.63	0.45
Vegetation	197.11	54.72	178.99	49.69	158.79	44.08	137.09	38.06	148.70	41.28
Open land	28.90	8.02	23.36	6.48	26.08	7.24	6.13	1.70	13.59	3.77
Agricultural land	115.77	32.14	133.23	36.99	147.90	41.06	188.32	52.28	169.14	46.96
Built-up area	14.90	4.14	21.64	6.01	25.22	7.00	26.86	7.46	27.16	7.54
Land Area	360.21	100	360.21	100	360.21	100	360.21	100	360.21	100

Table 3. Producer and User Accuracy of Classified Images

Class Name	2005		2011		2015		2020		2024	
	Producers (%)	Users (%)	Producers (%)	Users (%)	Producers (%)	Users (%)	Producers (%)	Users (%)	Producers (%)	Users (%)
Water bodies	100.00	66.67	100.00	100.00	100.00	100.00	100.00	100.00	100.00	100.00
Vegetation	54.55	100.00	100.00	100.00	100.00	100.00	100.00	100.00	100.00	100.00
Open land	75.00	50.00	66.67	100.00	66.67	66.67	100.00	83.33	66.67	100.00
Built-up area	10.00	83.33	100.00	66.67	100.00	100.00	85.71	100.00	100.00	83.33
Agricultural land	100.00	100.00	100.00	83.33	100.00	100.00	100.00	100.00	100.00	66.67

Table 4. Overall Accuracy Assessment Results of Classified Images

Year	Classification Accuracy (%)	Kappa Statistics	Representation
2005	75.00	0.75	High
2011	87.50	0.88	Very High
2015	91.67	0.92	Very High
2020	95.83	0.96	Very High
2024	87.50	0.88	Very High

Classification Accuracy Assessment

The hybrid classification approach achieved consistently high accuracy across the multi-temporal datasets (Table 3). Overall classification accuracy ranged from 75.00% in 2005 to 95.83% in 2020, with Kappa coefficients between 0.75 and 0.96 (Table 4), indicating strong agreement with reference data. The highest classification performance was achieved in 2020 (95.83%; $\kappa = 0.96$), while a decline was observed in 2024 (87.50%; $\kappa = 0.88$) (Dash et al., 2023).

The reduced accuracy in 2024 can be attributed to seasonal variability, atmospheric interference, and spectral confusion between open land and degraded or sparsely vegetated surfaces, which exhibit similar reflectance characteristics (Congalton, 1991; Lu et al., 2004). Increased landscape heterogeneity and mixed-pixel effects also contributed to misclassification between open and built-up surfaces, a common limitation in complex tropical environments (El-Ashmawy, 2021). Despite this decline, classification reliability remains acceptable for change detection ($\kappa > 0.80$), and future refinements may involve integrating multi-temporal NDVI and NDBI indices to further enhance class separability (Karan & Samadder, 2016).

Environmental and Hydrological Implications

The observed LULC transitions have likely altered the hydrological functioning of the Rejoso Watershed through several interacting mechanisms. First, the long-term reduction in vegetated cover from 54.72% in 2005 to 41.28% in 2024 implies diminished canopy interception and root-zone reinforcement, potentially weakening infiltration capacity and slope stability. Second, the substantial expansion of agricultural land, particularly up to 2020, indicates intensified soil disturbance over a broad area, increasing susceptibility to compaction, surface sealing, and erosion during peak rainfall events. Although agricultural land generally supports higher infiltration than bare surfaces, intensive cultivation on sloping terrain often reduces soil hydraulic conductivity and increases sediment yield relative to natural vegetation (Naha et al., 2021).

Third, the steady increase in built-up areas has expanded impervious surfaces in downstream zones, enhancing quickflow generation and shortening runoff response times. Together, vegetation loss, agricultural intensification, and urban expansion increase exposure to runoff, erosion, and flood risk, particularly where cultivation extends into uplands and impervious cover spreads across lowlands. These implications are consistent with hydrological evidence from comparable tropical basins, where increasing imperviousness and reduced natural cover amplify storm runoff and peak flows by 15–25% (Cuypers et al., 2023). The gradual decline in water bodies may further reduce surface

storage capacity in some sub-areas, limiting hydrological buffering during extreme events (Iqbal et al., 2022).

Comparative Analysis and Policy Implications

The LULC trajectory of the Rejoso Watershed broadly aligns with patterns observed in rapidly developing watersheds across Java, although its dominant transformation pathway differs from cases where urban conversion is the primary driver. In Rejoso, the most substantial long-term change is the pronounced increase in agricultural land from 32.14% to 46.96%, accompanied by a significant decline in vegetation from 54.72% to 41.28%. Built-up expansion, while continuous, remains moderate in magnitude (4.14% to 7.54%) relative to agricultural growth, indicating that agricultural intensification rather than urbanization alone has been the principal force reshaping the watershed (Naha et al., 2021).

Comparative evidence from other Indonesian watersheds, such as the Bedog sub-watershed, demonstrates that even modest increases in impervious surfaces can substantially alter runoff regimes (Mejía-Veintimilla et al., 2024). The Rejoso case further shows that large-scale conversion of vegetation to agriculture, particularly on steeper slopes, can be equally critical in amplifying runoff and sediment yield. Accordingly, effective management should integrate stricter downstream urban zoning with upstream slope-oriented interventions, including reforestation, agroforestry, and protection of recharge areas (Budiman et al., 2022; Yusoff & Muharam, 2015). Without integrated land-use regulation, continued agricultural encroachment into uplands and incremental urban expansion downstream may progressively erode hydrological resilience and increase flood and erosion risks (Banjara et al., 2024).

Conclusion

This study demonstrates substantial spatiotemporal land-use transformation in the Rejoso Watershed from 2005 to 2024, characterized by long-term agricultural expansion and non-linear vegetation dynamics. Agricultural land increased from 32.14% (115.77 km²) in 2005 to 46.96% (169.14 km²) in 2024, after peaking sharply in 2020, while vegetation declined from 54.72% (197.11 km²) to 41.28% (148.70 km²), reaching its minimum extent in 2020 before partially recovering by 2024. The most critical finding of this study is the pronounced short-term land-use reversal observed after 2020, during which approximately 3% of the watershed experienced vegetation recovery within only four years, accompanied by a simultaneous contraction of agricultural land. This non-linear shift departs from the commonly reported monotonic vegetation decline in rapidly developing tropical watersheds and highlights the dynamic and potentially reversible nature of land-use trajectories in Rejoso. Built-up areas continued to expand steadily from 4.14% to 7.54%, confirming ongoing urbanization pressures, particularly in downstream zones, while open land exhibited sharp contraction in 2020 followed by partial re-emergence in 2024, reflecting transitional clearing and short-term land abandonment. The consistently high classification accuracy (overall accuracy 87.5–95.8%; κ = 0.88–0.96) confirms the robustness of the hybrid Landsat-based approach for long-term LULC monitoring. From an environmental perspective, the combined legacy of vegetation loss prior to 2020 and subsequent partial recovery suggests both increased hydrological vulnerability during peak agricultural expansion and emerging opportunities for watershed rehabilitation. Sustaining Rejoso's ecological and hydrological functions therefore requires integrated land-use management that prioritizes upstream vegetation restoration, sustainable agricultural practices, and stricter downstream spatial zoning to limit impervious expansion and enhance long-term watershed resilience.

Acknowledgments

All authors would like to thank to all parties who has supported this research.

Author Contributions

Conceptualization, methodology, formal analysis, investigation, writing—original draft preparation, A.M.F.; software, data curation, visualization, A.M.F.; writing—review and editing, validation, supervision, project administration, E.S. and L.P. All authors have read and agreed to the published version of the manuscript.

Funding

This research received no external funding.

Conflicts of Interest

The authors declare no conflict of interest.

References

Aboelnour, M. A., Tank, J. L., Hamlet, A. F., Bertassello, L. E., Ren, D., & Bolster, D. (2024). A SWAT model depicts the impact of land use change on hydrology, nutrient, and sediment loads in a Lake Michigan watershed. *Modeling Earth Systems and Environment*, *11*(1). https://doi.org/10.1007/s40808-024-02259-x

Adhikari, S., Leigh, L., & Pathiranage, D. S. (2025). Pressure-Related Discrepancies in Landsat 8 Level 2 Collection 2 Surface Reflectance Products and Their Correction. *Remote Sensing*, *17*(10), 1676.

https://doi.org/10.3390/rs17101676

Aravena, R. A., Lyons, M. B., Roff, A., & Keith, D. A. (2021). A Colourimetric Approach to Ecological Remote Sensing : Case Study for the Rainforests of South-Eastern Australia. *Remote Sensing*, *13*(13), 2544. https://doi.org/10.3390/rs13132544

Bal, S. K., Pramod, V. P., Sandeep, V. M., Manikandan, N., Sarath Chandran, M. A., Subba Rao, A. V. M., Vijaya Kumar, P., Vanaja, M., & Singh, V. K. (2023). Identifying appropriate prediction models for estimating hourly temperature over diverse agro-ecological regions of India. *Scientific Reports*, *13*(1), 1–13. https://doi.org/10.1038/s41598-023-34194-9

Banjara, M., Bhusal, A., Ghimire, A. B., & Kalra, A. (2024). Impact of Land Use and Land Cover Change on Hydrological Processes in Urban Watersheds : Analysis and Forecasting for Flood Risk Management. *Geosciences*, *14*(2), 40. https://doi.org/10.3390/geosciences14020040

Budiman, L. S., Deviana, A., Miftahurridlo, M., Saputra, A., M., D., Sudrajat, S., Nurjani, E., & Rachmawati, R. (2022). Spatial Analysis of Sustainable Management Strategy in Bedog Sub-Watershed Based on Carrying Capacity of Agricultural Land. *Iop Conference Series Earth and Environmental Science*. https://doi.org/10.1088/1755-1315/1039/1/012038

Chavez, P. S., & others. (1996). Image-based atmospheric corrections-revisited and improved. *Photogrammetric Engineering and Remote Sensing*, *62*(9), 1025–1035. Retrieved from https://static1.1.sqspcdn.com/static/f/891472/15133582/1321370214637/Chavez_P.S._1996.pdf

Congalton, R. G. (1991). A review of assessing the accuracy of classifications of remotely sensed data. *Remote Sensing of Environment*, *37*(1), 35–46. https://doi.org/10.1016/0034-4257(91)90048-b

Cuypers, S., Nascetti, A., & Vergauwen, M. (2023). Land Use and Land Cover Mapping with VHR and Multi-Temporal Sentinel-2 Imagery. *Remote Sensing*, *15*(10), 2501. https://doi.org/10.3390/rs15102501

Dash, P., Sanders, S. L., Parajuli, P., & Ouyang, Y. (2023). Improving the Accuracy of Land Use and Land Cover Classification of Landsat Data in an Agricultural Watershed. *Remote Sensing*, *15*(16), 4020. https://doi.org/10.3390/rs15164020

El-Ashmawy, N. T. H. (2021). *Innovative Approach for Automatic Land Cover Information Extraction From LiDAR Data*. Ryerson University. Retrieved from https://rshare.library.torontomu.ca/ndownloader/files/28129038

Fajri, M., Iswandi, U., Barlian, E., Syah, N., Haria, T., & Putra, A. (2025). Analysis of the Impact of Land Cover Change in 2010-2024 on the Potential of Water Catchment Areas in the Arau Watershed. *Jurnal Penelitian Pendidikan IPA*, *11*(10), 325–333. https://doi.org/10.29303/jppipa.v11i10.12002

Groeneveld, D., Ruggles, T., & Gao, B.-C. (2024). Landsat-8/9 Atmospheric Correction Reliability Using Scene Statistics. *Remote Sensing*, *16*(12), 2216. https://doi.org/10.3390/rs16122216

Iqbal, M., Wen, J., Masood, M., Masood, M. U., & Adnan, M. (2022). Impacts of Climate and Land-Use Changes on Hydrological Processes of the Source Region of Yellow River, China. *Sustainability*, *14*(22), 14908. https://doi.org/10.3390/su142214908

Karan, S. K., & Samadder, S. R. (2016). Accuracy of Land Use Change Detection Using Support Vector Machine and Maximum Likelihood Techniques for Open-Cast Coal Mining Areas. *Environmental Monitoring and Assessment*. https://doi.org/10.1007/s10661-016-5494-x

Khafaji, R. G. A. H. Al, & Al-Zubaidi, E. A. (2024). Unsupervised Classification of Landsat-8 Satellite Imagery- Based on ISO Clustering. *Wasit Journal of Computer and Mathematics Science*, 40–53. https://doi.org/10.31185/wjcms.212

Lu, D., Mausel, P., Brondízio, E., & Moran, E. (2004). Change detection techniques. *International Journal of Remote Sensing*, *25*(12), 2365–2401. https://doi.org/10.1080/0143116031000139863

McFeeters, S. K. (1996). The use of the Normalized Difference Water Index (NDWI) in the delineation of open water features. *International Journal of Remote Sensing*, *17*(7), 1425–1432. https://doi.org/10.1080/01431169608948714

Mejía-Veintimilla, D., Ochoa-Cueva, P., & Arteaga-Marín, J. (2024). Evaluation of the Hydrological Response to Land Use Change Scenarios in Urban and Non-Urban Mountain Basins in Ecuador. *Land*, *13*(11), 1907. https://doi.org/10.3390/land13111907

Naha, S., Rico-Ramirez, M. A., & Rosolem, R. (2021). Quantifying the impacts of land cover change on hydrological responses in the Mahanadi river basin in India. *Hydrology and Earth System Sciences*, *25*(12), 6339–6357. https://doi.org/10.5194/hess-25-6339-2021

Octaviani, L. A., Cahyono, B. E., & Suprianto, A. (2025). Identification of Remote Sensing Data : NDVI , LST , and LULC on Geothermal Manifestations in Bondowoso Regency. *Jurnal Penelitian Pendidikan IPA*, *11*(4), 1039–1046. https://doi.org/10.29303/jppipa.v11i4.9620

Ode, L., Akbar, J., Djau, B., Djaba, A., Faradiba, C. D., & Yusuf, D. (2025). Spatial Changes in the Fluvial

Landscape of the Bone River and Socio-Economic Impacts through Geospatial Technology Integration (Landsat-GIS) in the Gorontalo Region. *Jurnal Penelitian Pendidikan IPA*, *11*(10), 312–324. https://doi.org/10.29303/jppipa.v11i10.12731

Ogato, G. S., Bantider, A., & Geneletti, D. (2021). Dynamics of Land Use and Land Cover Changes in Huluka Watershed of Oromia Regional State, Ethiopia. *Environmental Systems Research*. https://doi.org/10.1186/s40068-021-00218-4

Pandey, A., Bishal, K. C., Kalura, P., Chowdary, V. M., Jha, C. S., & Cerdà, A. (2021). A Soil Water Assessment Tool (SWAT) Modeling Approach to Prioritize Soil Conservation Management in River Basin Critical Areas Coupled With Future Climate Scenario Analysis. *Air, Soil and Water Research*, *14*. https://doi.org/10.1177/11786221211021395

Purwanto, A. (2023). Flood Risk Spatial Modeling Based on Geographical Information Systems and Remote Sensing in the Pemangkat Regensi. *Jurnal Penelitian Pendidikan IPA*, *9*(11), 9554–9563. https://doi.org/10.29303/jppipa.v9i11.5264

Quilbé, R., Rousseau, A. N., Moquet, J.-S., Savary, S., Ricard, S., & Garbouj, M. S. (2008). Hydrological responses of a watershed to historical land use evolution and future land use scenarios under climate change conditions. *Hydrology and Earth System Sciences*, *12*(1), 101–110. https://doi.org/10.5194/hess-12-101-2008

Rachman, F., Huang, J., Xue, X., & Marfai, M. A. (2024). Insights from 30 Years of Land Use/Land Cover Transitions in Jakarta, Indonesia, via Intensity Analysis. *Land*, *13*(4). https://doi.org/10.3390/land13040545

Sadhwani, K., Eldho, T. I., & Jha, M. K. (2022). Effects of Dynamic Land Use / Land Cover Change on Flow and Sediment Yield in a Monsoon-Dominated Tropical Watershed. *Water*. https://doi.org/10.3390/w14223666

Singh, A. (1989). Review Article Digital change detection techniques using remotely-sensed data. *International Journal of Remote Sensing*, *10*(6), 989–1003. https://doi.org/10.1080/01431168908903939

Singh, B., Sihag, P., & Singh, K. (2018). Comparison of Infiltration Models in NIT Kurukshetra Campus. *Applied Water Science*. https://doi.org/10.1007/s13201-018-0708-8

Surbakti, H., Salsabilah, R., Aryawati, R., & Sitepu, R. (2025). Utilization of Google Earth Engine and DSAS to Monitor Coastal Change in the Banyuasin Estuary. *Jurnal Penelitian Pendidikan IPA*, *11*(6), 252–262. https://doi.org/10.29303/jppipa.v11i6.10922

Vahreza, A., Isa, M., & Zaini, N. (2024). Analysis of the Distribution of Carbon Monoxide Gas and Nitrogen Dioxide Gas and Urban Heat Island (UHI) Based on Multi-Temporal Satellite Data During the Implementation of the. *Jurnal Penelitian Pendidikan IPA*, *10*(2), 6790–6797. https://doi.org/10.29303/jppipa.v10i9.8593

Vigiak, O., Malagó, A., Bouraoui, F., Vanmaercke, M., & Poesen, J. (2015). Adapting SWAT hillslope erosion model to predict sediment concentrations and yields in large Basins. *Science of The Total Environment*, *538*, 855–875. https://doi.org/10.1016/j.scitotenv.2015.08.095

Xu, X., Ji, X., Jiang, J., Yao, X., Tian, Y., Zhu, Y., Cao, W., Cao, Q., Yang, H., Shi, Z., & Cheng, T. (2018). Evaluation of One-Class Support Vector Classification for Mapping the Paddy Rice Planting Area in Jiangsu Province of China From Landsat 8 OLI Imagery. *Remote Sensing*. https://doi.org/10.3390/rs10040546

Yang, S., Zhao, W., Liu, Y., Wang, S., Wang, J., & Zhai, R. (2018). Influence of land use change on the ecosystem service trade-offs in the ecological restoration area: Dynamics and scenarios in the Yanhe watershed, China. *Science of The Total Environment*, *644*, 556–566. https://doi.org/10.1016/j.scitotenv.2018.06.348

Yang, Y., Yang, D., Wang, X., Zhang, Z., & Nawaz, Z. (2021). Testing Accuracy of Land Cover Classification Algorithms in the Qilian Mountains Based on GEE Cloud Platform. *Remote Sensing*. https://doi.org/10.3390/rs13245064

Yesuph, A. Y., & Dagnew, A. B. (2019). Land use / cover spatiotemporal dynamics, driving forces and implications at the Beshillo catchment of the Blue Nile Basin , North Eastern Highlands of Ethiopia. *Environmental Systems Research*. https://doi.org/10.1186/s40068-019-0148-y

Yusoff, N. M., & Muharam, F. M. (2015). The Use of Multi-Temporal Landsat Imageries in Detecting Seasonal Crop Abandonment. *Remote Sensing*. https://doi.org/10.3390/rs70911974

Zha, Y., Gao, J., & Ni, S. (2003). Use of normalized difference built-up index in automatically mapping urban areas from TM imagery. *International Journal of Remote Sensing*, *24*(3), 583–594. https://doi.org/10.1080/01431160304987

Zhang, C., Chen, X., Shao, H., Chen, S., Liu, T., Chen, C., Ding, Q., & Du, H. (2018). Evaluation and Intercomparison of High-Resolution Satellite Precipitation Estimates—GPM, TRMM, and CMORPH in the Tianshan Mountain Area. *Remote Sensing*. https://doi.org/10.3390/rs10101543